

Charge and sodium ordering in $\text{Na}_{0.33}\text{V}_2\text{O}_5$

Raman and optical spectroscopy

P. H. M. van Loosdrecht^y, C. N. Presura, M. Popinciuc, D. van der Marel, G. Maris and T. T. M. Palstra

Material Science Center, University of Groningen, Nijenborgh 4, 9747 AG Groningen, The Netherlands

P. J. M. van Bentum

University of Nijmegen, Toernooiveld, 6525 ED Nijmegen, The Netherlands

H. Yamada, T. Yamachi and Y. Ueda

Institute for Solid State Physics, University of Tokyo, Japan

April 14, 2024

Abstract. Polarized Raman and optical spectra for the quasi-one dimensional metallic vanadate $\text{Na}_{0.33}\text{V}_2\text{O}_5$ are reported for various temperatures. The spectra are discussed in the light of the sodium and charge ordering transitions occurring in this material, and demonstrate the presence of strong electron-phonon coupling.

Keywords: charge ordering, metal-insulator transition, vanadates, phase transitions, Raman and optical spectroscopy

1. introduction

The recent discovery [1] of a clear metal-insulator transition (MIT) in the vanadium bronze $\text{Na}_{0.33}\text{V}_2\text{O}_5$ has sparked a revival of interest in this quasi one-dimensional metallic system. In addition to the MIT,

^y (p.van.loosdrecht@phys.rug.nl)



$\text{Na}_{0.33}\text{V}_2\text{O}_5$ undergoes a structural sodium ordering transition at higher temperatures, a magnetic transition at low temperatures, and a transition into a superconducting state under high pressure [2]. Several important aspects of this 1D material have remained unclear, including the nature of the spin and charge excitations, and the relation between the Na ordering and the MIT. This contribution presents a Raman and optical study of $\text{Na}_{0.33}\text{V}_2\text{O}_5$ focusing on the various phase transitions and electron phonon coupling in this compound.

2. Structure and phase transitions

At room temperature $\text{Na}_{0.33}\text{V}_2\text{O}_5$ has a monoclinic structure (spacegroup C_{2h}^2 , $a = 10.08 \text{ \AA}$, $b = 3.61 \text{ \AA}$, $c = 15.44 \text{ \AA}$, $\beta = 109.6^\circ$) [3, 4]. The structure consists of zigzag double chains of VO_6 octahedra, forming sheet by joining corners. These sheets are separated by additional chains of double VO_5 trigonal bipyramids, giving rise to unidirectional tunnels along b (see Fig. 5) in which the Na ions are located. At a sodium stoichiometry of 0.33, there is exactly one sodium atom per primitive cell. The sodium ion can occupy two closely spaced positions, although simultaneous occupation of the two sites is prohibited (the distance between the sites is 1.95 \AA). NMR experiments [5] suggest that, at room temperature, the occupation of these two sites is random giving rise to a disordered structure. At $T = 240 \text{ K}$ a second order phase transition occurs in which the sodium atoms order in a zigzag fashion along the unique axis accompanied by a doubling of the b -axis [1]. Two additional transitions occur at lower temperatures. At $T = 136 \text{ K}$ a metal-insulator transition has been observed, in which the unit cell undergoes an additional tripling along the b -axis [6]. It has been suggested that the charge ordering occurs due to a localization of the charge

on chains along the b-direction formed by the V_1 ions. Finally, at $T \approx 22$ K there is a transition from the paramagnetic high temperature state to a canted antiferromagnetic state [7]

3. Raman spectroscopy

The samples used in this study have been prepared as described in [1]. Typical sizes are 5–6 mm along the b-direction and about 0.3–1 mm in the other two directions. For the Raman experiments, samples were mounted in a flow cryostat (stabilization better than 1 K). Polarized spectra have been recorded in a back reflection geometry using an Ar⁺ ion laser (514 nm) for excitation (power < 5 mW, spot size 100 μm) and a state of the art triple pass Raman spectrometer with diode array detection. Typical spectra are shown in figure 5 (left part).

Due to the low symmetry and the large number of atoms in the unit cell, the spectra show a large number of active phonon modes in all symmetries. What immediately draws attention is the large width of most of the observed phonon modes. In particular in the 400–800 cm^{-1} region, the line widths are 10–50 cm^{-1} . The active phonons here are expected to be vanadium–oxygen bending modes. This strong broadening is believed to be due to a strong electron phonon coupling, consistent with a polaronic picture of the electronic properties of this material [8, 9]. The coupling is then a result of the modulation of the hopping parameters for O (2p)–V (3d) hopping by the phonons.

A group theoretical analysis shows that the room temperature $k=0$ optical phonons can be classified as $\Gamma = 11A_u + 22B_u + 20A_g + 10B_g$, in which the gerade modes are Raman active (A_g in (aa), (bb), (cc), and (ac), and B_g in (ab) and (bc) polarization) and the ungerade IR active (A_u for b polarization, B_u for a

and c polarizations). Consistent with the crystal symmetry 16 modes are observed in A_g symmetry, and 9 in B_g symmetry. The missing modes might be too weak to be observed, but might also escape detection due to near degeneracy.

Below the sodium ordering transition the crystal structure adheres to a C_{2h}^5 [6, 10] symmetry. The symmetry analysis leads now to a decomposition $\Gamma = 65A_u + 64B_u + 66A_g + 66B_g$ for the optical modes. Experimentally 55 modes are observed in A_g symmetry, and 20 in B_g symmetry. Below the charge ordering transition the unit cell triples, leading to about 190 active phonons for each irreducible representation. Although a few phonons seem to be activated below the metal-insulator transition, the spectra do not show this tripling. Again, this might be due to a lack of scattering strength or near degeneracies.

The strongest changes in the spectra are observed below the metal-insulator transition at $T = 136$ K. This is exemplified in figure 5 (right panel). Apparently, the localization of the electrons leads to a decrease of the coupling of the phonons to electronic excitations.

4. optical spectroscopy

Temperature dependent optical constants of $Na_{0.33}V_2O_5$ in the NIR-UV range ($6000\text{--}35000\text{ cm}^{-1}$) have been measured using ellipsometry on a surface containing the b-axis. In addition the reflectivity spectra have been measured as a function of temperature and polarization in the IR-MIR range ($20\text{--}6000\text{ cm}^{-1}$). The optical conductivity of $Na_{0.33}V_2O_5$ has been determined by combining the reflectivity data with the ellipsometric data and performing a Kramers-Kronig analysis [9]. The room temperature results are shown in figure 5.

The strong absorption band observed above 10000 cm^{-1} in both spectra is due to charge transfer excitations from the oxygen 2p to the vanadium 3d levels, similar as has been observed in NaV_2O_5 [11]. The optical conductivity $\sigma(\omega)$ b-axis shows an absorption band around 8000 cm^{-1} , again similar to what is observed in NaV_2O_5 . This band is probably due to a bonding-antibonding transition on the $\text{V}_1\text{-O-V}_3$ bonds [9].

At lower energy the one dimensional metallic nature of $\text{Na}_{0.33}\text{V}_2\text{O}_5$ is clearly demonstrated by the finite spectral weight for $E \rightarrow 0$ for a polarization along the b-axis, and the tendency to zero weight in the perpendicular polarization. Indeed the data can be fitted by a Drude model, yielding an unscreened plasma frequency of $\omega_p \approx 3200\text{ cm}^{-1}$, and a scattering time $\tau \approx 40\text{ ps}$. This low energy response has been attributed to mobile small polarons. The from the optical data estimated DC conductivity is $200\text{ }\Omega^{-1}\text{ cm}^{-1}$, which compares well to the published DC conductivity of $100\text{ }\Omega^{-1}\text{ cm}^{-1}$ [1]. Another manifestation of the polaronic nature of $\text{Na}_{0.33}\text{V}_2\text{O}_5$ is found in the characteristic [12] absorption peak around 3000 cm^{-1} .

At room temperature one expects a total of 32 active phonon modes, 11 in A_u symmetry (polarization along b), and 22 in B_u symmetry (\perp b). Along the insulating direction (figure 5, lower curve) we indeed observe 22 active phonon modes. In contrast, the metallic direction (figure 5, upper curve) exhibits only two strong phonon modes, all other modes appear as strongly broadened weak features in the spectrum, indicating again the importance of electron phonon coupling in this material. Already below the sodium ordering transition one expects many new phonon modes, though only few are actually observed (for an example see figure 5 lower right panel). In contrast, the metal insulator transition leads to a spectacular gradual appearance of a large number of phonon modes (see figure 5, upper and lower left panels). The observed behavior is reminiscent of the observation of phase- or charged phonons in several charge density wave materials, resulting from electron-phonon interactions [13].

5. conclusions

The Raman and optical spectra presented in this contribution demonstrate in many ways the importance of electron-phonon coupling in $\text{Na}_{0.33}\text{V}_2\text{O}_5$. The observed phonon modes and symmetry are found to be in overall agreement with the phase transitions in this material, although the appearance of the many modes in the IR spectra along the metallic direction probably does not result from symmetry breaking, but rather gain strength from electron-phonon coupling in the charge ordered phase. Finally, one interesting undiscussed aspect of the optical data is the appearance of a continuum and Fano distortions of phonon modes (see figure 5 upper panel). The origin of this low energy continuum is presently unknown, but likely to be of electronic nature.

Acknowledgements

This work was partially supported by the Dutch Foundation for Fundamental Research on Matter (FOM) and by INTAS (99-155).

References

1. H. Yamada and Y. Ueda, J. Phys. Soc. Jpn. 68, 2735 (1999).
2. T. Yamachi, Y. Ueda, N. Mori, unpublished (2002).
3. A. D. Wadsley, Acta Cryst. 8, 695 (1955).
4. H. Kobayashi, Bull. Chem. Soc. Japan 52, 1315 (1979).
5. K. Murayama and H. Nagasawa, J. Phys. Soc. Jpn. 48, 2159 (1980).
6. J.-I. Yamaura, M. Isobe, H. Yamada, T. Yamachi, Y. Ueda, J. Phys. Chem. Sol. (2002, in press).
7. A. N. Vasil'ev, I. M. archenko, A. I. Smimov, S. S. Sosin, P. L. Kapitza, H. Yamada and Y. Ueda, Phys. Rev. B 64, 174403 (2001).
8. N. F. Mott, Metal-insulator transitions, Taylor and Francis, 1974.
9. C. Presura, M. Popinciuc, P. H. M. van Loosdrecht, D. van der Marel, M. Mostovoy, G. M. aris, T. T. M. Palstra, H. Yamada, and Y. Ueda, cond-mat/02xxxxx (2002).
10. G. M. aris et al., unpublished (2002).
11. C. Presura, D. van der Marel, M. Dischner, C. Geibel, and R. K. Krenner, Phys. Rev. B 62, 16522 (2000).
12. C. A. Kuntscher, M. Dressel, F. Lichtenberg, J. Mannhart, D. van der Marel, Y. Kanai, S. Kagoshima and H. Nagasawa, cond-mat/0205049; D. Emin, Phys. Rev. B 48, 13691 (1993); D. Kaplan and A. Zylbersztein, J. de Physique 37, L-123 (1976)
13. M. J. Rice, Phys. Rev. Lett. 37, 36 (1976); L. Degiorgi, P. Wachter, C. Schlenker, Physica B 164 (1990), 305, and references therein.

Figure captions

1. Room temperature structure of $\text{Na}_{0.33}\text{V}_2\text{O}_5$ showing chains of V_1 (dark octahedra), V_2 (light octahedra), and V_3 ions (pyramids).
2. left: Polarized Raman spectra of $\text{Na}_{0.33}\text{V}_2\text{O}_5$ for $T = 15\text{ K}$ and 300 K . Upper panel A_g ($b\bar{b}$), middle panel A_g ($b\bar{b}$), lower panel B_g ($b\bar{b}$) symmetry. right: Detailed temperature dependence of the $400\text{--}800\text{ cm}^{-1}$ region of the A_g ($b\bar{b}$) Raman spectrum. In all panel the subsequent curves have been given an offset for clarity.
3. Optical conductivity of $\text{Na}_{0.33}\text{V}_2\text{O}_5$ at room temperature calculated from reflectivity spectra (FIR-MIR) and ellipsometric data (MIR-UV). [9].
4. upper panel: Optical conductivity of $\text{Na}_{0.33}\text{V}_2\text{O}_5$ along the metallic direction above and below the charge ordering transition. lower panels: Phonon modes appearing below the sodium (c) and charge ordering (b) transitions. The inset shows the temperature dependence of the phonons shown in panels b) and c).

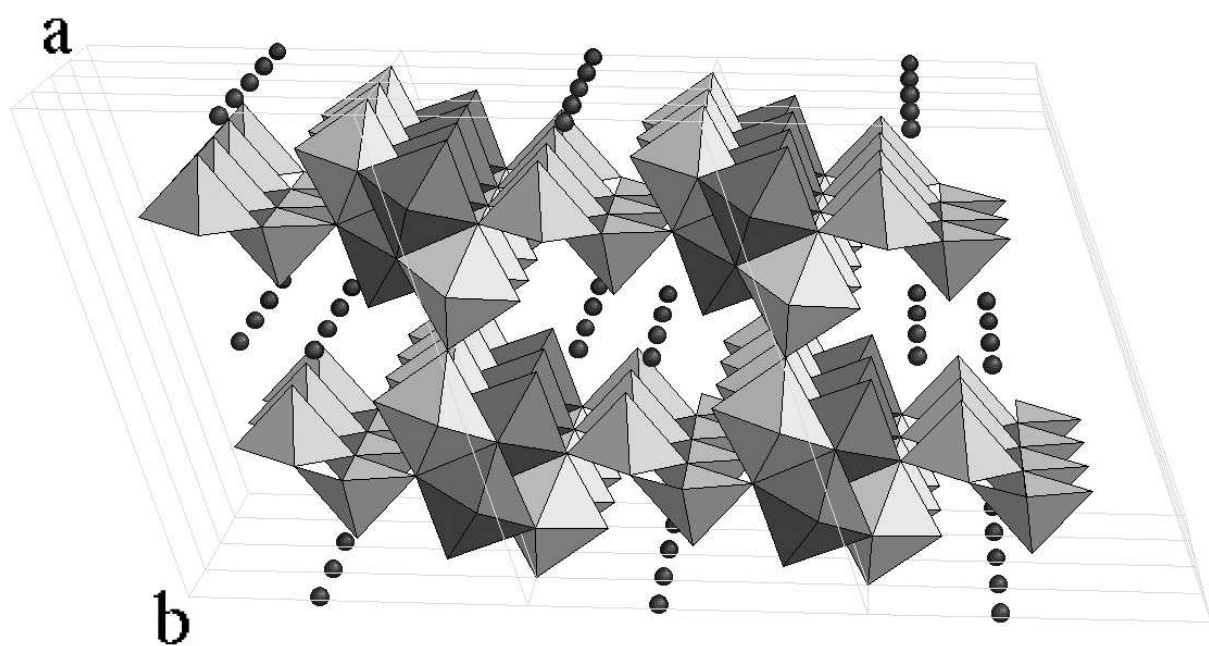
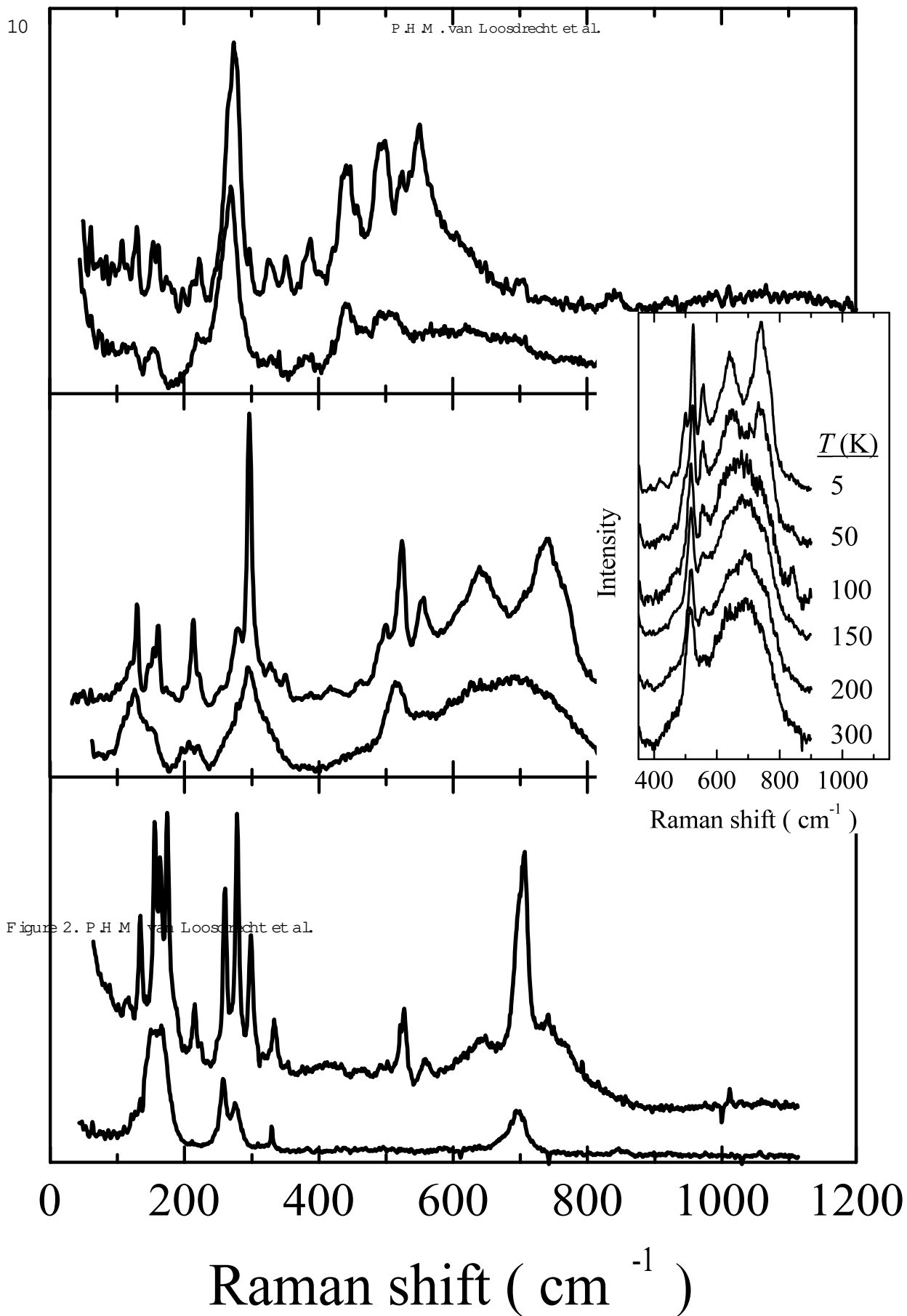


Figure 1. P. H. M. van Loosdrecht et al.

Intensity



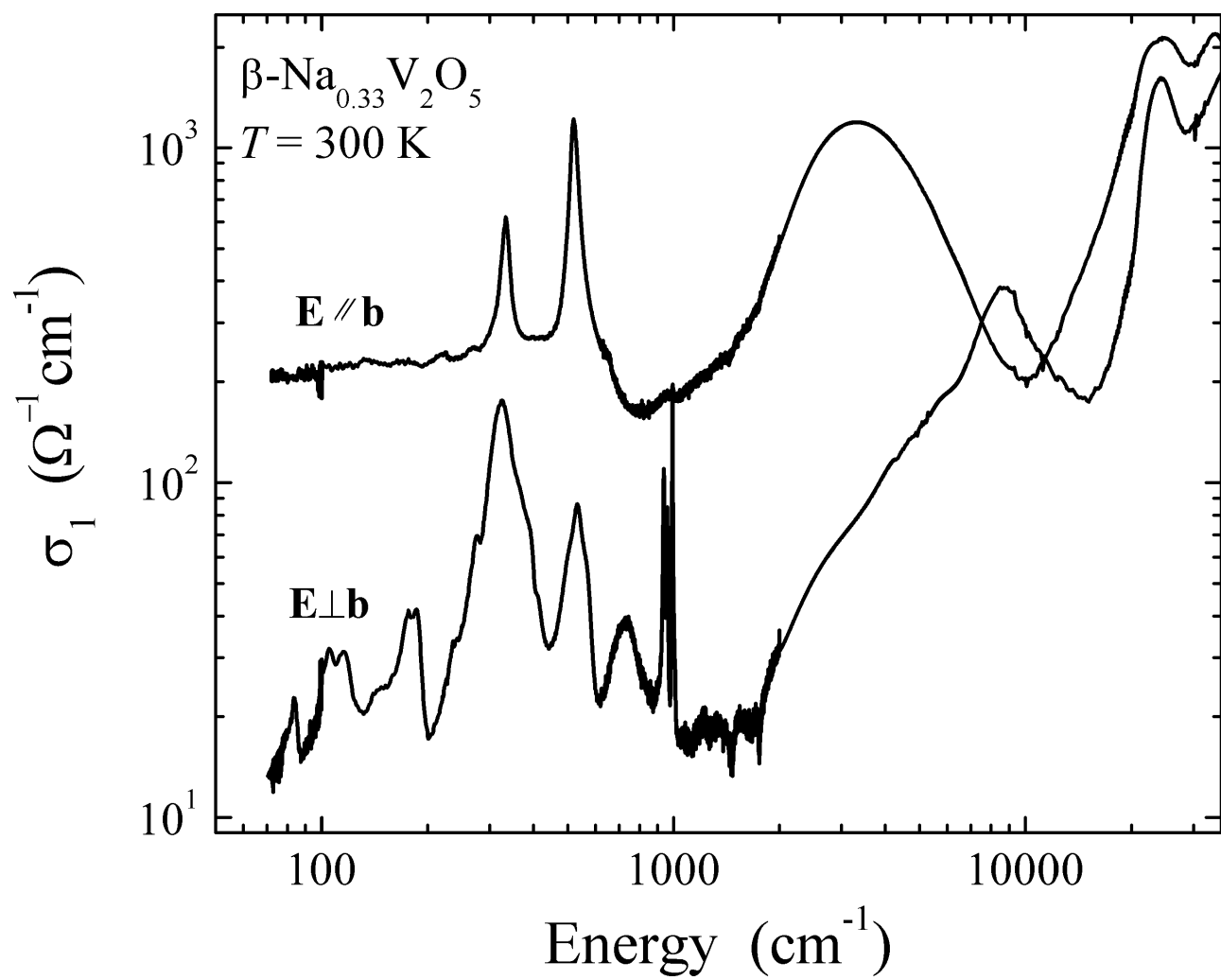


Figure 3. P. H. M. van Loosdrecht et al.

Address for Oprints:

P. H. M. van Loosdrecht

University of Groningen

Nijenborgh 4

9747 AG Groningen

The Netherlands

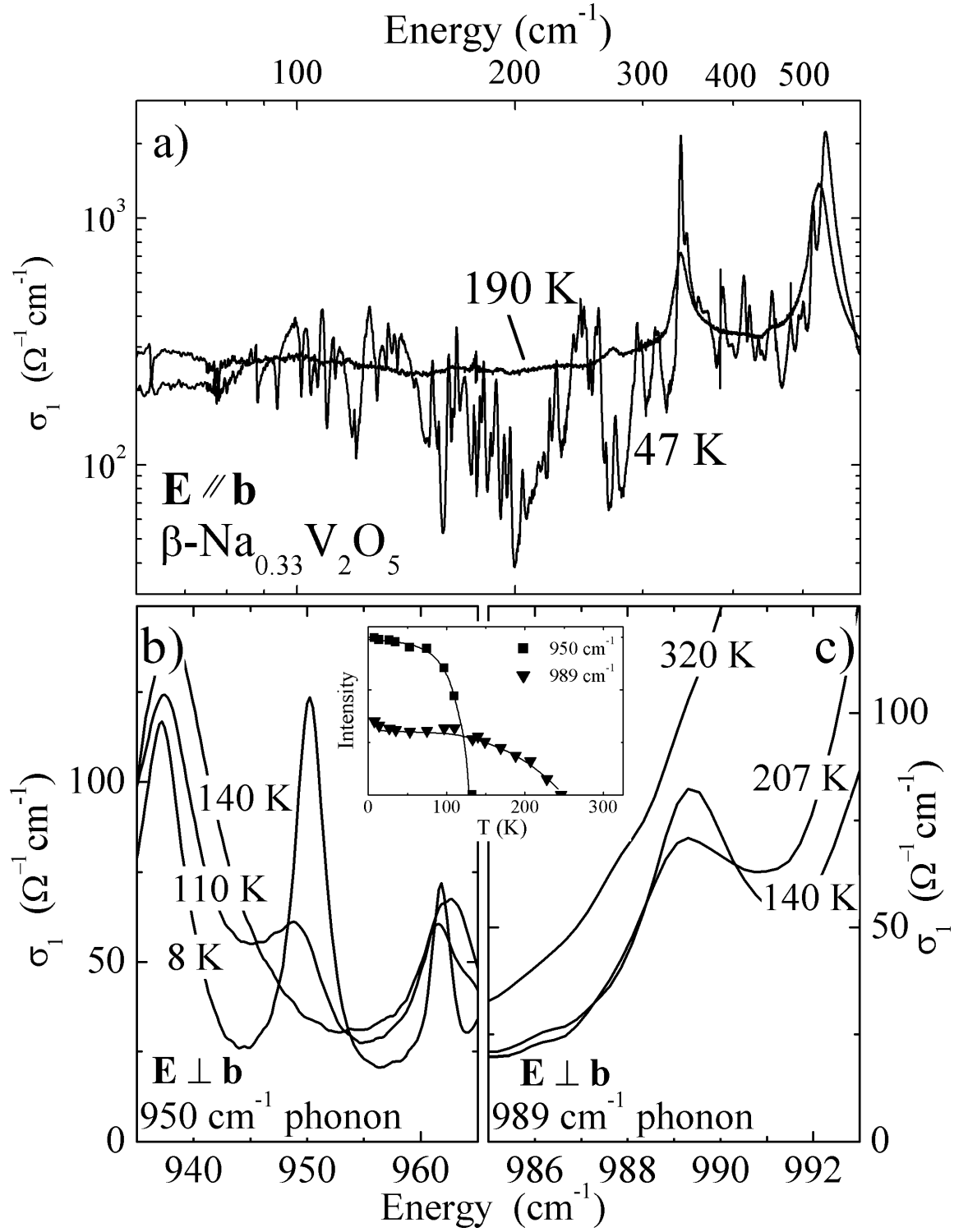


Figure 4. P. H. M. van Loosdrecht et al.

